JMEPEG (2001) 10:173-177 ©ASM International

A Study of Fusion Zone Microstructures of Arc-Welded Joints Made from Dissimilar Aluminum Alloys

C.C. Menzemer, P.C. Lam, C.F. Wittell, and T.S. Srivatsan

(Submitted 24 November 1999; in revised form 14 October 2000)

Arc welding has proven itself to be an economically affordable and efficient method for the joining of a wide variety of aluminum alloy structures that find extensive use in the industries of ground transportation and building construction. Welded joints, having a "T" configuration, in dissimilar aluminum alloys were produced using the semiautomatic arc welding process. In this study, a combination of a non-heat-treatable aluminum-magnesium alloy and a heat-treatable aluminum-magnesium-silicon alloy was successfully welded. Optical microscopy was used to characterize the fusion zone microstructures of the fillet-welded T joints. The intrinsic microstructural features and the development and presence of defects are highlighted.

Keywords alloy 5083-H321, alloy 6061-T6, gas metal arc welding (GMAW), microstructures, weld fusion zone

1. Introduction

Gas metal arc welding (GMAW) has been successfully used for the joining of a variety of aluminum alloy structures for well over five 5 decades. Besides, a spectrum of welded products and structures finding use in the aerospace industry, other typical applications that make extensive use of aluminum and aluminum alloys span the industries of ground transportation and building construction.[1] A few notable examples include (a) covered hopper railcars, (b) coal cars for unit train service, (c) intermodal shipping containers, and (d) automobile frames. In the building construction industry, a wide spectrum of aluminum alloy products find use for the building of curtain walls, domed roof systems, and overhead sign trusses. Arc welding, and specifically GMAW, provides an energy efficient and concentrated heat source necessary for the development of joints that require deep penetration, narrow heat-affected zones (HAZs), and enhanced overall efficiency.[2,3] Furthermore, GMAW can be executed at relatively high speeds, while concurrently maintaining joint quality, integrity, and efficiency at acceptable levels.[2] These process attributes coupled with economic affordability provide the much-needed impetus for enhancing shop productivity.[1,2]

Key characteristics that exert an influence on GMAW welding of aluminum alloys include the following: (1) presence of a surface oxide coating, (2) shield gas used, (3) metal transfer mode, (4) solubility of gaseous hydrogen at temperatures approaching the molten state, (5) single versus multiple passes, (6) electrode position, (7) filler metal diameter, (8) shrinkage upon solidification, and (9) relatively high thermal and electrical conductivity.[4–6] Since the melting point of the aluminum oxide is much higher than that of the base metal, production-welding processes must be capable of breaking up the oxide film, while concurrently facilitating cleaning. As the oxide behaves as an insulator, fusion of the metal becomes difficult once the oxide layer is allowed to thicken. Furthermore, the oxide coating is porous and serves as an attractive trap for moisture, dirt, grease, and oils. This intrinsic feature of the oxide film coupled with the affinity of molten aluminum for gaseous hydrogen tends to promote the presence of porosity in weldments. Consequently, this necessitates the need for the aluminum alloy surfaces, adjacent to the joint region, to be clean and dry prior to welding. Cleaning of the aluminum alloys prior to welding consisted of essentially two steps. Initially, the surfaces of the joint area were wiped with an organic solvent. Light manual abrading of the joint and the adjacent areas using a stainless steel wire brush followed this. This assists in breaking up the oxide deposit and concurrently ensuring adequate fusion and penetration. An analysis of microstructural development of the welded joints, particularly at the (a) fusion zone, (b) fusion boundary, and (c) HAZ, is important in the determination of properties of the welded joint and overall joint integrity and soundness.

This paper presents and discusses the microstructures resulting from semiautomatic welding of two dissimilar aluminum alloys. The conjoint influence of welding technique and heat input on the presence and distribution of fine microscopic defects and the development of intrinsic microstructural features is highlighted.

2. Material and Sample Preparation

The material chosen for the flange of the "T" joint configuration was Al-Mg-Si alloy 6061-T6, while that of the stem or web was Al-Mg alloy 5083-H321. Precise chemical composition of the two alloys is given in Table 1. These two alloys have been proven in a wide spectrum of industrial applications to form a readily weldable combination. Samples were welded using mechanized torch travel and probe seam tracking. Semiautomatic welding was accomplished using a constant voltage (CV) power supply. The constant voltage power supply facilitates in maintaining a constant arc length. Variation in torch-to-work

C.C. Menzemer, Department of Civil Engineering, and **P.C. Lam, C.F. Wittel,** and **T.S. Srivatsan.** Department of Mechanical Engineering, College of Engineering, The University of Akron, Akron, OH 44325. Contact e-mail: tsrivatsan@uakron.edu.

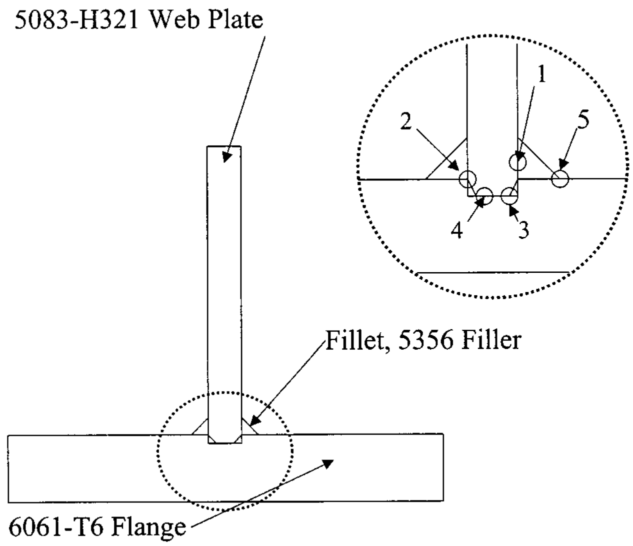

Fig. 1 Schematic of the T joint made from 6061-T6 flange and 5083-H321 web

Table 1 Chemical composition (wt.%) of the aluminum alloys 6061 and 5083

Alloy	Si	Fe	Cu	Mn	Mg	Cr	Zn	Ti	Al
6061	0.4	0.7	0.4	0.15	1.0	0.2	0.25	0.15	Bal
5083	0.4	0.4	0.1	0.4	4.0	0.10	0.25	0.15	Bal

piece distance tends to cause significant changes in current with concomitant influence on penetration. The filler material used was wire stock of aluminum alloy 5356. A schematic of the T joint is exemplified in Fig. 1.

The fusion zone microstructures were characterized by optical microscopy. Samples for metallography preparation were wet ground on progressively finer grades of silicon carbide impregnated emery paper, using copious amounts of water as the lubricant. Subsequently, the ground samples were mechanically polished using 5 and 1 m alumina-based polishing compound suspended in distilled water. Grain morphology and other intrinsic microstructural features were revealed using Keller's reagent (a solution mixture of hydrofluoric acid + nitric acid + hydrochloric acid + distilled water) as the etchant. The etched samples were observed in an optical microscope and photographed using a standard bright-field illumination technique.

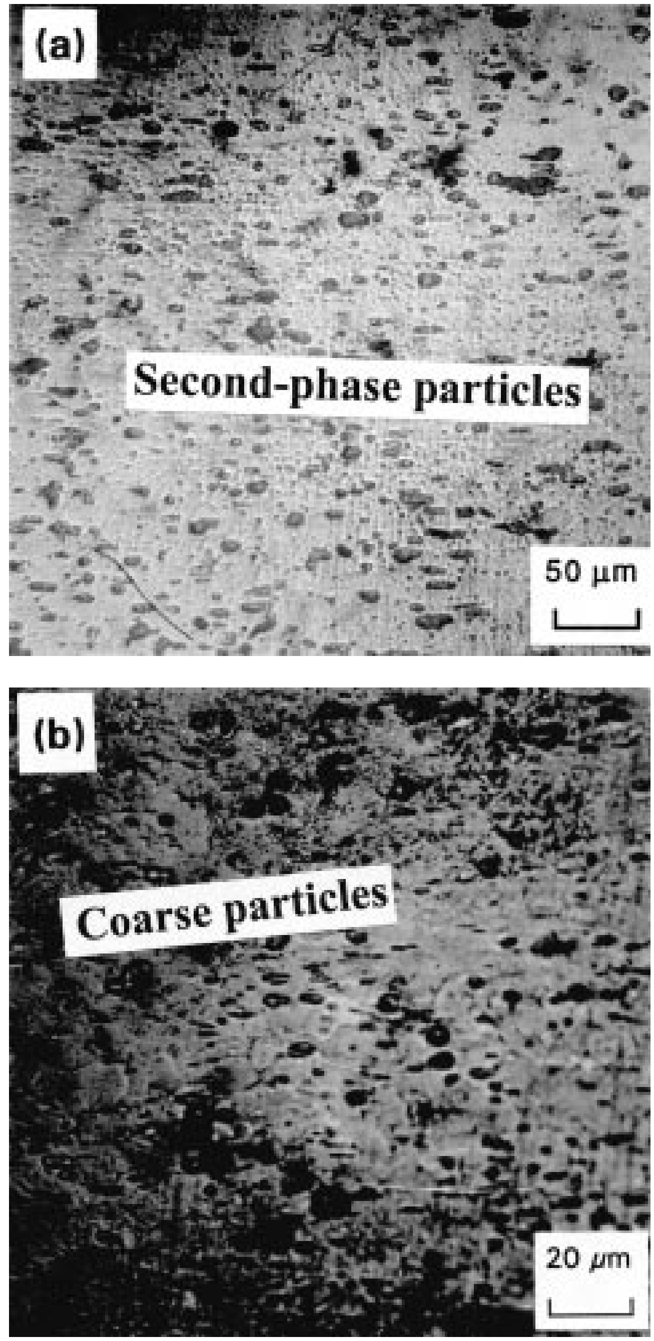

Fig. 2 (**a**) and (**b**) Bright-field optical micrographs showing distribution of the coarse and intermediate size particles in aluminum alloy 6061-T6

3. Results and Discussion

3.1 Initial Microstructure of As-Received Alloys

The presence of iron as an impurity element in aluminum alloy 6061-T6 results in the precipitation of a high volume fraction of coarse iron-rich and even silicon-rich constituents during conventional casting. These particles have been identified to be compounds of A_7Cu_2Fe and $Al_{12}(FeMn)_3Si$[7,8] and range in size from about 3 to 10 m (Fig. 2). The presence of chromium as the grain refining elements results in the precipitation of dispersoids ($Al_{12}Mg_2Cr$) during ingot preheat and high-temperature homogenization treatments.[8] The chromium dispersoids aid in retaining the directional grain structure developed during mechanical deformation (extrusion) of the flange product, while assisting in preventing the excessive growth of the recrystallized grains that form during subsequent heat treatments. Copper is added primarily for the purpose of offering corrosion protection. Besides, copper has limited solubility in aluminum and precipitates as a ternary compound (Al_2CuMg) during ingot solidification and preheating.[9,10] Silicon and magnesium are present in balance to form the quasi-binary Al-Mg_2Si. Strengthening in the alloy arises from the presence of the magnesium silicide phase β(Mg_2Si), which is the primary hardening precipitate formed during artificial aging of the alloy at temperatures ranging from 433 to 463 K. A ratio of magnesium to available silicon of 1.7:1 ensures that almost all of the solute is contained in the Mg_2Si phase.[8] The excess silicon in the alloy, over and above the amount required for the formation of the ordered Mg_2Si phase, is deposited at the grain boundaries as elemental silicon. The alloy is fully recrystallized with fairly large grains flattened in the primary extrusion or longitudinal direction (L). Clustering of the coarse second-phase particles was observed resulting in particle-rich and particle-depleted regions. The coarse second-phase particles were also found decorating the grain boundaries.

The amount of magnesium (4.0%) present in alloy 5083-H321 is higher than that retained in solid solution at room temperature.[9] Because of the low solubility of the Mg_2Si phase in pure aluminum at high magnesium contents, it is often present in the microstructure as the major constituent.[9] The magnesium in solution imparts limited solid solution strengthening to the aluminum alloy matrix besides facilitating additional strengthening through its influence on work hardening. The conjoint influence of magnesium in solution and the strain hardening arising from cold deformation are responsible for the acceptable strength of this alloy. Besides second-phase particles containing iron, manganese and silicon are also present. The presence of manganese results in the precipitation of dispersoids (Al_6(MnFe)) during the ingot preheat and high-temperature homogenization treatments. Manganese in solution facilitates in decreasing the recrystallized grain size, thereby enhancing strength. In wrought stock, the ternary compound $Al_{12}Mg_2Cr$, referred to as the "E" phase, precipitates during ingot preheat. The unwelded microstructure of the 5083-H321 reveals fully recrystallized grain structure with nonuniform distribution of coarse second-phase particles throughout the microstructure (Fig. 3).

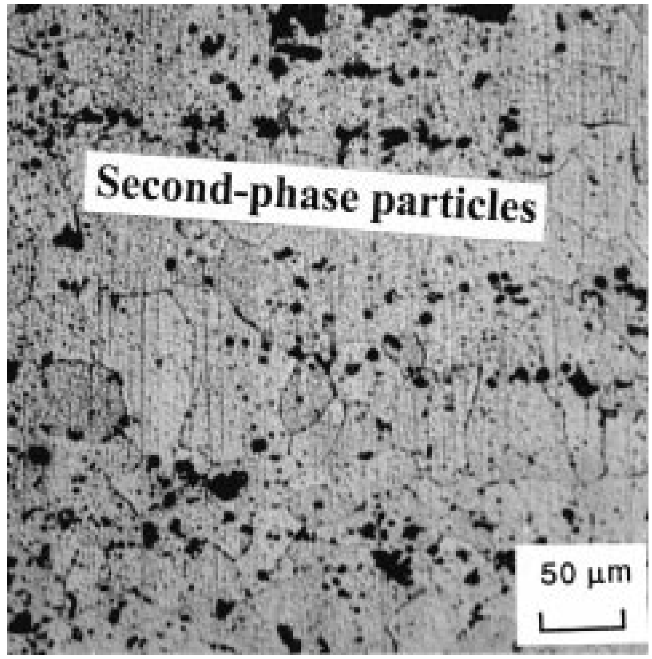

Fig. 3 Bright-field optical micrograph showing particle distribution and grain morphology in aluminum alloy 5083-H321

3.2 Fusion Zone Microstructures

The microstructure of the welded region was examined for joints welded by the semiautomatic technique. Figure 4(a) shows the microstructure at the interface of the 5083-H321 web plate and weld fusion line (region 1 in Fig. 1). A cast structure is readily apparent at the weld bead. Grains of the parent 5083 material, immediately adjacent to the fusion line, show evidence of coarsening coupled with segregation of the coarse second-phase particles to the boundaries.

The microstructure at the intersection of the 5083-H321 web plate with the 6061-T6 flange (region 2 in Fig. 1) is shown in Fig. 4(b). The weld bead reveals a cast microstructure. The coarse and intermediate-size second-phase particles and other constituents have segregated to the grain boundaries of the parent material, immediately adjacent to the weld fusion line. The grains at and adjacent to the fusion line revealed evidence of coarsening. The coarsening and segregation of the microstructure are attributed to the heat generated during the welding process.

Figure 4(c) reveals the microstructure at the interface of the 6061-T6 flange and the 5083-H321 web (region 3 in Fig. 1). Both the 5083 web plate and the 6061 flange are in contact with each other and not in direct contact with the weld bead. The heat of welding was found to have a minor influence on intrinsic microstructural features. Few of the grains revealed evidence of coarsening coupled with segregation of the coarse constituents and other second-phase particles to the interface.

The microstructure at the interface between the web and flange plate, along the bottom of the recess, is shown in Fig. 4(d). The 5083-H321 web and 6061-T6 flange maintain contact with each other, and not under the immediate influence of the weldment. Since the last part of the Al-Mg containing weld to solidify would be the center, a magnesium-rich aluminum would segregate to this region. This is confirmed by the evidence of segregation, presence, and clustering of the second-phase particles at and along the grain boundaries of the 5083-H321-alloy web plate. Such segregation and concomitant clustering are attributed to be the conjoint influence of heat generated during welding and its influence on the kinetics of solidification. Furthermore, numerous fine microscopic cracks were observed along the grain boundaries of the 6061-T6 flange, both at and adjacent to the interface.

The microstructure of the 6061-T6 flange immediately adjacent to the weld toe (region 5 in Fig. 1) is shown in Fig. 5. Numerous fine and microscopic "hot-short" cracks were observed. The presence and occurrence of the hot-short cracks suggests the generation and concomitant influence of heat retention during semiautomatic welding. Furthermore, in the case of this alloy, the thermal excursions in the HAZ will eradicate the prior thermo-mechanical processing (TMP) history, causing the second phases to resolutionize and reprecipitate at and along the grain boundaries. This segregation and precipitation would tend to weaken boundary strength. The intrinsic differences in localized stress state exacerbate cracking in this region.

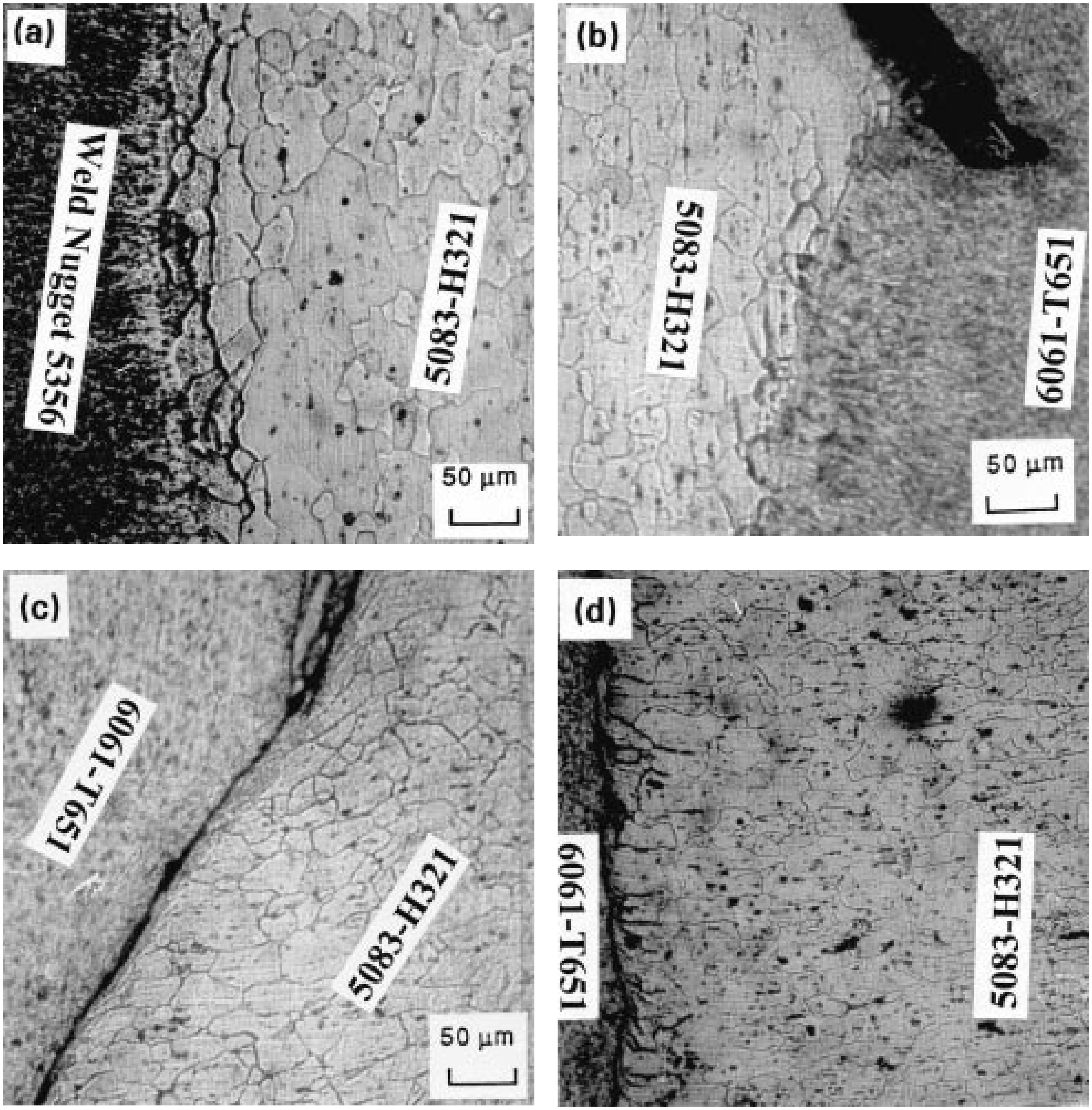

Fig. 4 Bright-field optical micrographs of the T joint showing microstructural features (**a**) adjacent to the fusion line and the 5083-H321 web (region 1 in Fig. 1), (**b**) at the intersection of the 5083-H321 web and the 6061-T6 flange (region 2 in Fig. 1), (**c**) at the interface between the 5083-H321 web and 6061-T6 flange (region 3 in Fig. 1), and (**d**) at the bottom of the T joint (region 4 in Fig. 1)

Coarsening of the recrystallized grains, immediately adjacent to the weld bead, at all locations of the T joint is largely influenced by the rate of cooling. The relatively slow dissipation of residual heat results in coarsening of the grains. Larger grains result in reduced boundary contact area and enhance the susceptibility to solidification cracking. Solidification mechanics can be used to account for the observed segregation and clustering of the coarse second-phase particles as well as changes in grain size. Both the solidification growth rate (R) and the temperature gradient (G) are two key parameters along with solute concentration, which determines the microstructure of the weld fusion zone. The observed characteristics may be attributed to a large G/R ratio.

4. Conclusions

Based on the examination of the microstructure of the fusion zone of dissimilar aluminum alloy joints fabricated by the semi-

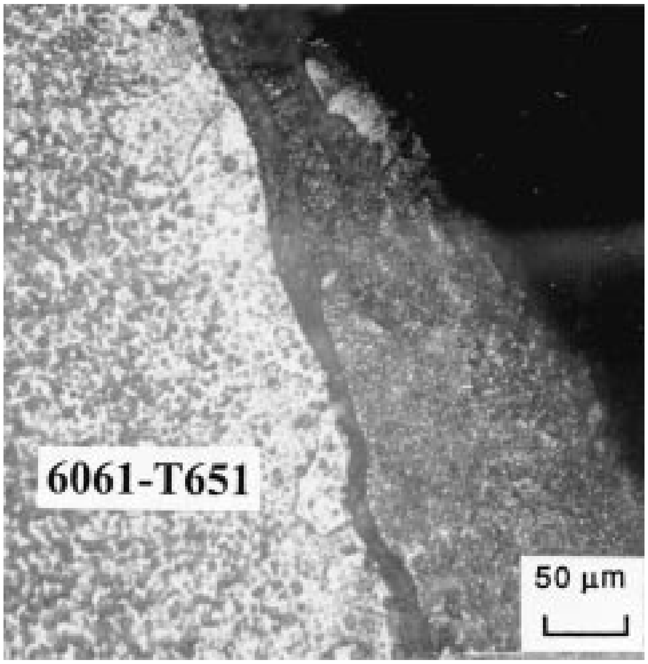

Fig. 5 Bright-field optical micrograph of the fusion zone microstructure adjacent to the weld toe on the 6061 flange (region 5 in Fig. 1)

automatic technique of GMAW, the following observations can be made.

- Grains of the parent material close to the fusion line show coarsening of the microstructure, as evidenced by the enlargement of grains and segregation of second-phase particles to the grain boundaries.
- Coarsening of the local microstructure may be attributed to the heat generated during the welding process.
- Hot-short cracks were observed near the weld toe on the 6061-T6 extruded flange. Occurrence of eutectic melting or hot-short cracking suggests that local heat input was fairly large coupled with the existence of localized stress states caused by the remelting and nonuniform distribution of second-phase particles.

Acknowledgments

The authors extend sincere thanks to The University of Akron for partial support of this research through a tuition scholarship.

References

1. C. Menzemer: *Aluminum Alloys and the Infrastructure*, Chapter 4, "Emerging Materials for Civil Infrastructure", ASCE, R.A. Lopez-Anido, and T.R. Naik, eds., 2000, pp. 115-34.
2. *Welding Aluminum: Theory and Practice*, Technical Advisory Panel on Welding and Joining, The Aluminum Association, Washington, DC, 1992.
3. "Welding of ALCOA Aluminum Alloys," Internal Technical Report, Aluminum Company of America, Pittsburgh, PA, 1972.
4. R. Martukanitz: *ASM Metals Handbook*, vol. 6, *Welding, Brazing and Soldering*, ASM International, Materials Park, OH, 1993.
5. P. Dickerson: *ASM Metals Handbook*, vol. 6, *Welding, Brazing and Soldering*, ASM International, Materials Park, OH, 1993.
6. M.L. Sharp: *Behavior and Design of Aluminum Structures*, McGraw-Hill, New York, NY, 1992.
7. E.A. Starke, Jr.: *Mater. Sci. Eng.*, 1977, vol. 29, pp. 99-115.
8. E.A. Starke, Jr.: in *Aluminum Alloys: Contemporary Research and Applications*, A.K. Vasudevan and R.H. Doherty, eds., Academic Press, New York, NY, 1989, p. 35.
9. R.E. Sanders, Jr., S.F. Baumann, and H.C. Stumpf: *Aluminum Alloys: Contemporary Research and Applications*, Academic Press, New York, NY, 1989, pp. 65-90.
10. D. Altenpohl: *Aluminum Viewed from Within*, Aluminum Verlag, Dusseldorf, 1982.